Brain Pathology ISSN 1015-6305

RESEARCH ARTICLE

Phosphorylated NUB1 distinguishes α-synuclein in Lewy bodies from that in glial cytoplasmic inclusions in multiple system atrophy

Kunikazu Tanji[1]; Yasuo Miki[1]; Fumiaki Mori[1]; Tomoya Kon[1]; Akiyoshi Kakita[2]; Hitoshi Takahashi[2]; Koichi Wakabayashi[1]

[1] Department of Neuropathology, Institute of Brain Science, Hirosaki University Graduate School of Medicine, Hirosaki, Japan.
[2] Department of Pathology, Brain Research Institute, University of Niigata, Niigata, Japan.

Keywords
α-synuclein, dementia with Lewy bodies, Lewy body disease, multiple system atrophy, NUB1, Parkinson's disease, phosphorylation, Synucleinopathy.

Corresponding author:
Kunikazu Tanji, Department of Neuropathology, Hirosaki University Graduate School of Medicine, 5 Zaifu-cho, Hirosaki 036-8562, Japan
(E-mail: *kunikazu@hirosaki-u.ac.jp)*

Received 10 October 2018
Accepted 15 April 2019
Published Online Article Accepted 21 April 2019

doi:10.1111/bpa.12728

Abstract

Posttranslational modifications by phosphorylation, ubiquitination, neddylation and other pathways have emerged as major regulators of cellular functions. NEDD8 ultimate buster 1, NUB1, is an adaptor protein, which negatively regulates the levels of the ubiquitin-like protein NEDD8 as well as neddylated proteins through proteasomal degradation. We previously reported that NUB1 is highly involved in the pathogenesis of synucleinopathy including Parkinson's disease (PD), dementia with Lewy bodies (DLB) and multiple system atrophy (MSA). In general, since phosphorylation is strongly related to the alteration of protein propensity, we examined if the fundamental function of NUB1 can be modulated by its phosphorylation. We created a series of phosphomimic mutants of NUB1. Among them, we found that phosphorylation of NUB1 at S46 (P-NUB46) efficiently degrades aggregates using a cell-based assay. Immunohistochemical studies have shown that specific antibodies against P-NUB46 reacted with Lewy bodies in PD and DLB but not with glial cytoplasmic inclusions in MSA. Moreover, P-NUB46 levels were significantly higher in the brains of patients with DLB than in control brains, and P-NUB46 was extracted in an insoluble fraction of DLB. These findings suggest that the phosphorylation of NUB1 is modulated during the pathological process of Lewy body disease.

INTRODUCTION

Neurodegenerative diseases are characterized by the aggregation of specific molecules, especially α-synuclein, which is aggregated in the brains of patients with Parkinson's disease (PD), dementia with Lewy bodies (DLB) and multiple system atrophy (MSA), which are called synucleinopathies. α-Synuclein is physiologically a presynaptic protein that is solubilized with Triton X-100 and proteinase K (PK) treatment. By contrast, abnormal α-synuclein tends to aggregate formation and is resistant to Triton X-100 and PK. This alteration of α-synuclein propensity can be mainly attributed to posttranslational modifications such as phosphorylation, nitration and ubiquitination (1, 2, 4). In particular, α-synuclein is abnormally phosphorylated at the 129th serine residue (S) and phosphorylated α-synuclein at S129 has been widely used as a pathological hallmark of synucleinopathy (1).

NUB1 was originally isolated as an interacting protein of NEDD8, which is one of the ubiquitin-like proteins (6). NUB1 possesses an ubiquitin-like (UBL) domain at its N-terminus and two ubiquitin-associated (UBA) domains at its C-terminus. A splicing variant, NUB1L, has three UBA domains (12). Interestingly, NUB1 homologues of other species such as mouse (accession number: AF534114), Drosophila (accession number: AE003752) and Arabidopsis (accession number: AC007295) have three UBA domains. Although NUB1L possesses a higher binding affinity with ubiquitinated proteins relative to NUB1, both NUB1 and NUB1L (collectively referred to as NUB1) bind to NEDD8 and ubiquitinated proteins. NUB1 overexpression has been shown previously to reduce neddylated proteins (6, 12). Moreover, NUB1 degrades ubiquitin C, synphilin-1, tau and mutant Hungtingtin (Htt) (7, 11, 13, 18), suggesting that NUB1 may play a role in certain neurodegenerative diseases, especially since both NUB1 and synphilin-1 are localized to α-synuclein-positive Lewy bodies (LBs) as well as to glial cytoplasmic inclusions (GCIs) in MSA (15, 19, 20). More importantly, we showed that NUB1 coexists with abnormal PK-resistant α-synuclein in LB disease patients and Tg mice expressing α-synuclein A53T. Collectively, these findings suggest a strong association of NUB1 with abnormal α-synuclein (16).

In the present study, we created several phosphomimic mutants of NUB1 and found that its phosphorylation

differently degrades disease-associated aggregates consisting of abnormal Htt by a cell-based assay. Among these NUB1 mutants, we focused on the phosphorylation of NUB1 at S46 (P-NUB46), which exhibited the greatest impact on the degradation of aggregates and cell-viability. Using our specific antibody against P-NUB46, we found that NUB1 is indeed phosphorylated at S46 in the brain, and P-NUB46 levels are significantly higher in DLB brains than in control brains. Additionally, a phospho-specific antibody against P-NUB46 reacted with LBs in PD and DLB but not GCIs or neuronal cytoplasmic inclusions in MSA. These findings suggest that P-NUB46 potentially distinguishes α-synuclein aggregates of LB disease from that of MSA.

MATERIALS AND METHODS

Subjects

Tissue samples were obtained from the Department of Neuropathology, Institute of Brain Science, Hirosaki University Graduate School of Medicine, Hirosaki and the Department of Pathology, Brain Research Institute, University of Niigata, Niigata, Japan. Written informed consent for autopsy, collection of samples and subsequent analysis was obtained from the next of kin of the deceased subjects who were involved in this study. This study was approved by the Committee of Medical Ethics of Hirosaki University Graduate School of Medicine, Hirosaki, Japan. Brain tissues from patients with PD (five male; age 70.0 ± 4.9; n = 5), DLB (five female and five male; age 74.2 ± 5.2; n = 10), MSA (two female and six male; age 73.1 ± 5.1; including MSA-C (n = 7) and MSA-P (n = 1) and aged-matched normal controls (two female and eight male; age 71.1 ± 8.4; n = 10) were used (Table 1). The diagnoses were confirmed by neuropathological examinations using immunohistochemistry for α-synuclein. There were not statistical differences in age, gender variables and post-mortem interval in hours among groups (Figure S1).

Cell culture and transfection

HeLa cells (Japanese Collection of Research Bioresources Cell Bank, Osaka, Japan) were maintained in Dulbecco's modified Eagle's medium supplemented with 10% fetal calf serum and antibiotics. Cultured cells were transfected with

Table 1. Summary of the human subjects examined. Abbreviations: PD = Parkinson's disease; DLB = dementia with Lewy bodies; MSA-C = multiple system atrophy cerebellar type; MSA-P = multiple system atrophy parkinsonism type; PMI = post-mortem-interval in hours.

No.	Analysis	Pathological diagnosis	Age (year)	Gender	PMI	Cause of death
1	Immunohistochemistry	Normal	53	M	9	Sudden death
2		Normal	75	M	1	Bronchopneumonia
3		Normal	80	F	2.5	Myocardial infarction
4		Normal	84	M	10	Sepsis
5		Normal	64	M	3	Acute tubular necrosis
6		PD	67	M	2	Bronchopneumonia
7		PD	63	M	4	Atelectasis
8		PD	69	M	1	Bronchopneumonia
9		PD	75	M	4	Pulmonary edema
10		PD	76	M	5.5	Bronchopneumonia
11		DLB	74	M	2.5	Bronchopneumonia
12		DLB	82	F	1	Aspiration pneumonia
13		DLB	78	M	3	Drowned
14		DLB	66	M	4	Bronchopneumonia
15		DLB	77	F	2	Bronchopneumonia
16		MSA-C	69	M	3	Bronchopneumonia
17		MSA-P	83	F	2	Aspiration pneumonia
18		MSA-C	66	M	2	Aspiration pneumonia
19	Biochemistry	Normal	71	M	1.5	Bronchopneumonia
20		Normal	76	M	3.5	Gastric bleeding
21		Normal	71	M	4	Aspiration pneumonia
22		Normal	72	M	3	Sudden death
23		Normal	64	F	2	Pulmonary hemorrhage
24		DLB	66	M	4	Bronchopneumonia
25		DLB	75	F	1.5	Aspiration pneumonia
26		DLB	70	F	3	Aspiration pneumonia
27		DLB	74	M	2.5	Bronchopneumonia
28		DLB	80	F	4	Bronchopneumonia
29		MSA-C	72	M	3.5	Aspiration pneumonia
30		MSA-C	75	M	4	Sudden death
31		MSA-C	70	M	3	Bronchopneumonia
32		MSA-C	78	M	3	Sudden death
33		MSA-C	71	M	4	Aspiration pneumonia

the following cDNAs: Flag-NUB1, α-synuclein, enhanced green fluorescent protein (EGFP)-synphilin-1 or pathological CAG-repeat length (Q74; plasmid 40262) of the Huntingtin exon 1 (Addgene, Cambridge, MA, USA) (8). After a 24-h incubation, cells were observed using a microscope (Eclipse Ti, Nikon, Tokyo, Japan) equipped with a 20 x objective lens, a spinning disc system (TI-S-EJOY, Nikon) and a CCD camera (CoolSNAP HQ2, Photometrics, Tucson, AZ, USA), or using a FlexStation3 (Molecular Devices, Sunnyvale, CA) for measuring EGFP intensity in cells. For immunoblotting analysis, cells were harvested at the indicated time and lysed as indicated below.

Primary antibodies

For generation of antibodies against phosphorylated NUB1 at S46, rabbits were immunized with a synthetic peptide based on residues 40–52 of human NUB1 conjugated at the amino terminus by an additional cysteine to the keyhole limpet hemocyanine together with adjuvants (Scrum Inc., Tokyo, Japan). Antisera were purified by obtaining flow-through fractions from a column conjugated with the NUB1 peptide. Specificity of phosphorylated NUB1 was characterized by enzyme-linked immunosorbent assay (ELISA) via plating the immunogen peptide in multiwell plates. To demonstrate the specificity, the rabbit antisera against P-NUB46 were preabsorbed with a phosphorylated peptide. After centrifugation, the supernatant was filtered and used for the experiments. For immunohistochemical studies, treatment with alkaline phosphatase (NEB, Beverly, MA, USA) was also performed before incubation with the primary antibody.

The following antibodies were used in this study. Mouse monoclonal antibodies against α-synuclein (4D6; Santa Cruz Biotechnology, Santa Cruz, CA, USA), Ubiquitin (FK2; MBL, Nagoya, Japan), Flag (M2; Sigma, Saint Louis, MO, USA), phosphorylated α-synuclein (pSyn#64, WAKO, Osaka, Japan) and human α-synuclein (LB509; Abcam, Cambridge, UK) and rabbit polyclonal antibodies against β-actin (Sigma), phosphorylated α-synuclein (Abcam), GFP (Thermo Fisher Scientific Inc., Waltham, MA), LC3 (MBL) and NUB1 (Abcam; ProteinTech Group, Inc., Chicago, IL, USA as well as our own antibody (6)) were used in this study. Horseradish peroxidase-conjugated anti-mouse, anti-rabbit or anti-goat IgGs (Santa Cruz Biotechnology) were used as a secondary antibody for western blot analyses.

Cell viability assay

Cell viability was measured by 3-(4,5-di-methylthiazol-2-yl)-2,5-diphenyltetrazolium bromide (MTT) assay (Cell counting kit-8, Wako). In brief, MTT assay reagent was put into medium at 10-fold dilution and incubated for 60 minutes at 37°C, followed by measurement at 450 nm.

Filter trap assay

We modified the filter trap analysis as described previously (17). Briefly, the phosphorylated or non-phosphorylated peptides were diluted with TBS (Tris-HCl, pH 7.5, 150 mM NaCl) and applied to a 0.22-μm cellulose acetate membrane (Millipore) on a slot blot apparatus (Bio-Rad, Hercules, CA, USA) using a vacuum manifold. After washing with TBS containing 0.1% Triton X-100, the membrane was incubated with anti-phosphorylated NUB1 and pan-NUB1 antibodies and detected using the enhanced chemiluminescent (ECL) detection system as described above.

Fractionation of brain extracts

For biochemical analysis, brain tissues were dissected at autopsy and rapidly frozen at -70°C. Frozen tissues from the middle temporal cortex of patients with DLB (n = 5) and control subjects (n = 5) were weighed, and proteins were sequentially extracted with buffers of increasing detergent strength using a previously described protocol (14). Samples were briefly homogenized with 10 volumes of buffer A (10 mM Tris-HCl, pH 7.5, 1 mM EGTA, 10% sucrose, 0.8 M NaCl) and centrifuged (fraction I). Afterward, an equal volume of buffer A containing 2% Triton X-100 was added. The samples were then incubated for 30 minutes at 37°C and centrifuged at 100 000 × g for 30 minutes at 4°C (fraction II). The resultant pellet was homogenized in 5 volumes of buffer A with 1% Sarkosyl and incubated for 30 minutes at 37°C. The homogenate was then centrifuged at 100 000 × g for 30 minutes at room temperature (fraction III). The Sarkosyl-insoluble pellet was homogenized in 4 volumes of buffer A containing 1% 3-[(3-Cholamidopropyl) dimethylammonio] propanesulfonate (CHAPS) (Sigma) and centrifuged at 100 000 × g for 20 minutes at room temperature (fraction IV). The pellet was sonicated in 0.2 volumes of 8 M urea buffer (fraction V). The CHAPS-soluble fraction (fraction IV) usually contains less total protein than other fractions by this method. We subjected a constant volume of extract in each fraction to SDS-polyacrylamide gel electrophoresis (PAGE).

Immunohistochemistry

Immunohistochemical analysis was carried out using the above paraffin-embedded sections. The sections were then subjected to immunohistochemical processing using the avidin–biotin–peroxidase complex method with diaminobenzidine. Monoclonal antibodies against phosphorylated α-synuclein (pSyn#64) and pan-α-synuclein (4D6), human α-synuclein (LB509) and a polyclonal antibody against P-NUB46 were used. The immunolabeled sections were counterstained with hematoxylin.

Western blot analysis

For total cell lysate, we used a lysis buffer with 4% sodium dodecyl sulfate (SDS; 75 mM Tris-HCl, pH 6.8, 4% SDS, 25% glycerol, 5% β-mercaptoethanol) and passed the sample through a 21-gauge needle attached to a 1-ml syringe. After SDS-polyacrylamide gel electrophoresis, western blot

analysis was performed as described previously (22). Transfer and detection were carried out according to the protocol provided with the ECL or ECL prime detection system (Amersham Pharmacia Biotech, Piscataway, NJ, USA).

Quantitative analysis and statistical analysis

A semiquantitative analysis of protein levels was performed using ImageJ software provided by the NIH (Bethesda, MD, USA). All data are represented as the mean + standard deviation. The statistical significance was evaluated using one-way ANOVAs with Bonferroni's post hoc test to analyze more than three groups and Student's *t*-test to analyze two groups. Kruskal–Wallis test was used to compare proportions of gender valuables. A probability value of less than 0.05 ($P < 0.05$) was considered significant.

RESULTS

Phosphorylated NUB1 inhibits the formation of aggregates

We have previously shown that NUB1 suppresses the formation of LB-like inclusions composed of α-synuclein (18). Since NUB1 has more than 20 potential sites that can be phosphorylated, we examined the effect of phosphorylated NUB1 on the aggregation in this study. Based on the result of a homology search on NUB1 of other species, we selected a series of conserved regions and made seven phosphomimic NUB1 mutants (Figure 1A,B). Immunocytofluorescent study showed anti-Flag antibody stained the cytoplasm and nucleus of cells with wild-type or mutant NUB1 (Figure 1C,D). Based on our previous studies, we mainly used HttQ74 aggregation tagged with EGFP as a cell-based assay, because signals of HttQ74 aggregation were brighter than that of α-synuclein (Figure 1C,D). As a result, EGFP intensity was significantly lower in cells with NUB S46E than that in wild-type NUB1, suggesting that S46E mutant exerted a significant inhibitory effect on HttQ74 aggregation (Figure 1E). MTT assay showed that the NUB1 S46E mutant suppressed cell death induced with Htt toxicity (Figure 1F). Conversely, the NUB1 S46A mutant, which is a phospho-inactive mutant, did not exhibit any inhibitory activity on aggregation.

Specificity of the anti-P-NUB46 antibody

We next generated a specific antibody against P-NUB46 to investigate the physiological and pathological roles *in vivo*. The specificity of the anti-P-NUB46 antibody was assessed by ELISA, filter trap assay and western blot analysis. ELISA showed that the phosphorylated peptide was recognized by the anti-P-NUB46 antibody in a concentration-dependent manner, while the non-phosphorylated peptide did not react with the anti-P-NUB46 antibody, although the antisera and pre-absorbed antibody reacted with them (Figure 2A,B). Consistent with the ELISA results, the filter trap assay demonstrated that anti-P-NUB46 antibody clearly recognized the phosphorylated peptide but not the non-phosphorylated one (Figure 2C). Furthermore, a positive signal was detected in the cell lysate of the NUB1 S46E mutant by western blot analysis using the anti-P-NUB46 antibody (Figure 2D). Interestingly, endogenous α-synuclein levels were significantly lower in the cell lysate of NUB1 S46E mutants than in the other mutants (Figure 2D lower panel and 2E). Conversely, α-synuclein levels were significantly higher in the cell lysate of NUB1 S589E mutant. Collectively, these results verified the specificity of the anti-P-NUB46 antibody.

NUB1 is phosphorylated in control and LB specimens

Using the anti-P-NUB46 antibody, we systematically immunostained the human brain sections. Anti-P-NUB46 weakly immunostained the neuronal cytoplasm and dendrites in controls (Figure 3A,D,G). Additionally, anti-P-NUB46 immunolabeled the axons of the gray and white matters of the brain with and without neurodegenerative diseases (Figure 3B,G). Immunohistochemistry showed that cortical and brainstem LBs were positive for P-NUB46 (Figure 3B,E). Positive staining was eliminated using anti-P-NUB46 absorbed with P-NUB peptide corresponding to S46 (Figure 3C). We also confirmed that the positive staining were abolished with alkaline phosphatase treatment (Figure 3F). To verify the colocalization of P-NUB46 and α-synuclein in LBs, we performed double immunofluorescence, indicating that P-NUB46 was localized in LBs, which were positive for phosphorylated α-synuclein (Figure 3I,J). P-NUB46 was moderately expressed in the core of LBs, whereas phosphorylated α-synuclein was distributed in the outer portion of LBs. We also examined P-NUB46 immunoreactivity in the brains of patients with MSA and found no reactivity for GCIs or oligodendrocytes in MSA (Figure 3H). We could not find any P-NUB46-positive staining on neuronal cytoplasmic and nuclear inclusions in MSA. Therefore, the involvement of P-NUB46 seems to be characteristic of LBs rather than a common phenomenon in α-synuclein-containing inclusions.

P-NUB46 levels are increased in the brains of patients with DLB

In the human brain, we assessed the total amount of P-NUB46 protein. Immunoblotting revealed that endogenous P-NUB46 was detected in the brains of patients with DLB and in control subjects. Quantitative data indicated that P-NUB46 levels were approximately threefold higher in DLB than in control brains (Figure 4A,B). Further biochemical analysis showed that P-NUB46 was mainly extracted in Trion X-100-insoluble fractions (III, IV and V) in the brains of patients with DLB (Figure 4C,D). By contrast, both detergent-soluble and detergent-insoluble P-NUB46 were found in the control brains. Thus, P-NUB46 solubility in DLB brains was completely different than that in control brains. Finally, we

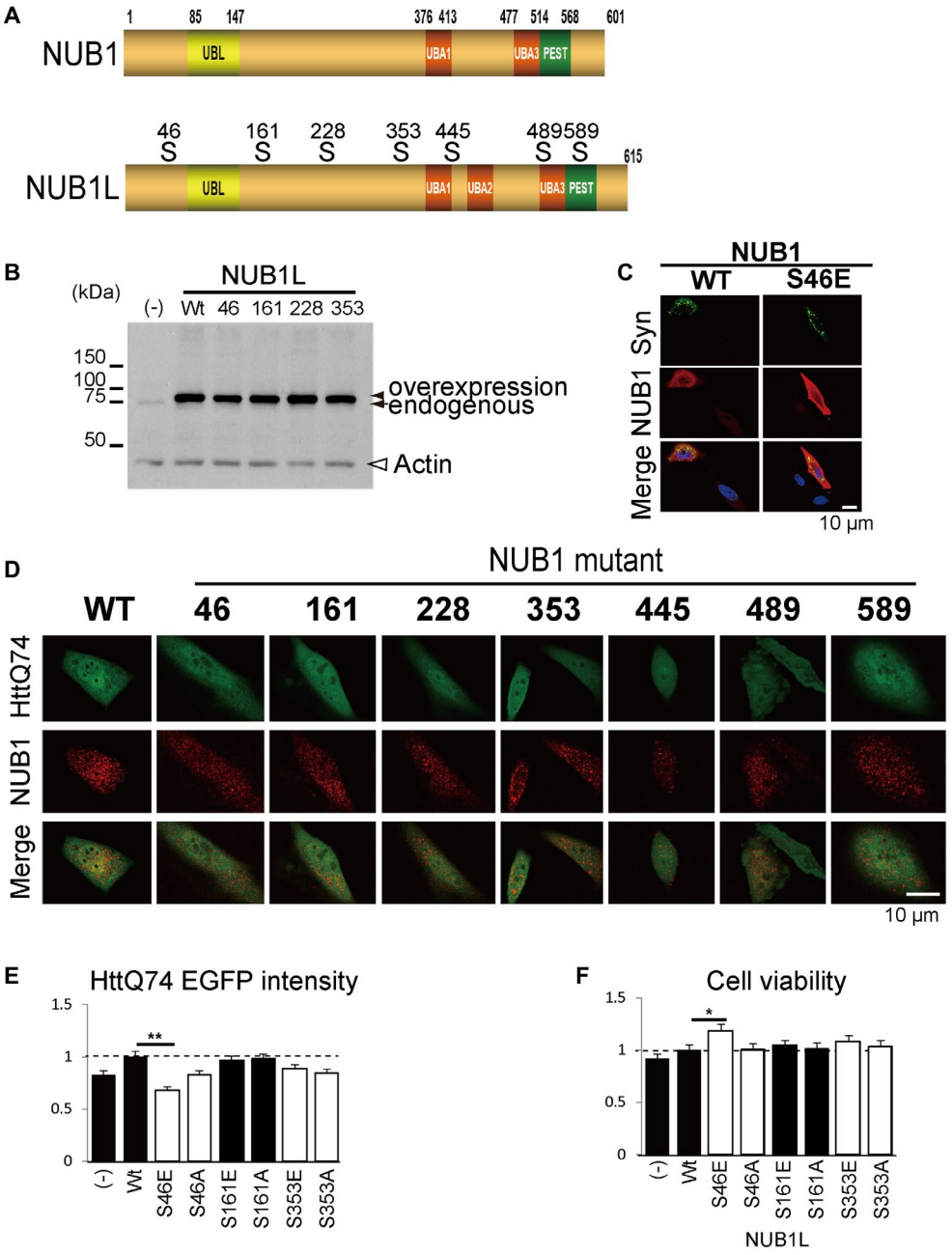

Figure 1. *Effect of phosphomimic NUB1 mutant on disease-causing protein aggregation.* **A.** Schematic representation of human NUB1 and NUB1L. NUB1 possesses an ubiquitin-like (UBL) and two ubiquitin-associated (UBA) domains as well as additional UBA domains in NUB1L. There are more than 20 serine residues (S) in NUB1/1L. Based on the homology search for NUB1 of other species, relatively higher conserved regions are selected and mutated S into E, which is a phosphomimic mutation. **B.** Western blot analysis shows almost equal levels of NUB1 mutants. Anti-NUB1 antibody detects endogenous NUB1 in cell transfected without a NUB1 construct (arrow), and arrowhead indicates overexpressed NUB1 and its mutant. **C,D.** HeLa cells were transfected with α-synuclein (Syn) or mutant huntingtin (Htt74Q) tagged with EGFP (green) together with NUB1 wild type or mutant as indicated (red). **E.** Among NUB1 mutants, NUB1 S46E significantly suppresses GFP signal of HttQ74. **F.** Quantitative data show that NUB1 suppresses EGFP signals using a FlexStation. NUB1 also recovers cell viability induced mutant Htt toxicity.

compared P-NUB46 levels in the cerebellar white matter of patients with MSA and controls. There was no difference in P-NUB46 levels between the MSA group and control group (Figure 4E,F). Double immunofluorescence showed that GCIs were not immunostained with anti-P-NUB46 antibody (Figure 4G).

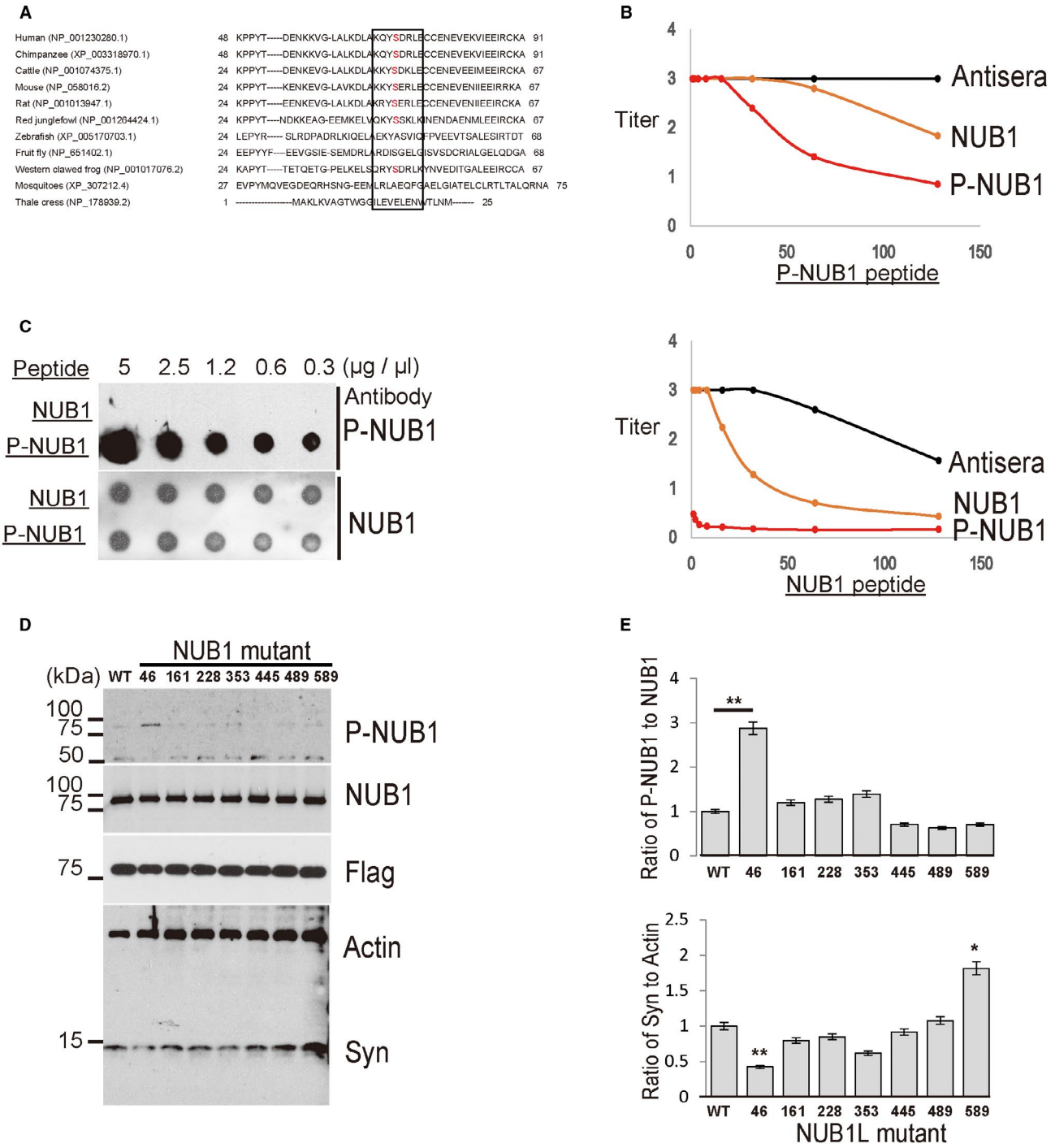

Figure 2. *Verification of antibody against phosphorylated specific NUB1 at S46 (P-NUB46).* **A.** Alignment of the regions around P-NUB46 and its homologues. Underlining represents the epitope for the antibody against P-NUB46. **B.** Enzyme-linked immunosorbent assay (ELISA) shows that anti-P-NUB46 antibody reacts with phosphorylated synthetic peptide (KQYSDRLE) in a concentration-dependent manner (upper panel). Non-phosphorylated synthetic peptide was diluted and reacted with anti-P-NUB46 antibody. Antisera and pre-absorbed antibody recognizes non-phosphorylated synthetic peptide, whereas anti-P-NUB46 antibody does not recognize it. **C.** Phosphorylated and non-phosphorylated synthetic peptide were used to confirm the reactivity of anti-P-NUB46 antibody by dot blot analysis. Anti-pan-NUB1 antibody reacts with peptides regardless of phosphorylation status. By contrast, anti-P-NUB46 antibody recognizes only phosphorylated peptide in a concentration-dependent manner. **D.** HeLa cells were transfected with each NUB1 phosphomimic mutant as indicated. Anti-P-NUB antibody clearly recognizes NUB1 phosphorylated at S46. The molecular mass is indicated on the left side of the panel. Anti-Flag antibody indicates equal amounts of NUB mutant to apply to the gel. Note that endogenous α-synuclein levels are significantly lower in cells with NUB S46E in relative to others. Conversely, α-synuclein levels are significantly higher in the cell lysate of NUB1 S589E mutant. **E.** Quantitative data of D. $*P < 0.05$, $**P < 0.01$.

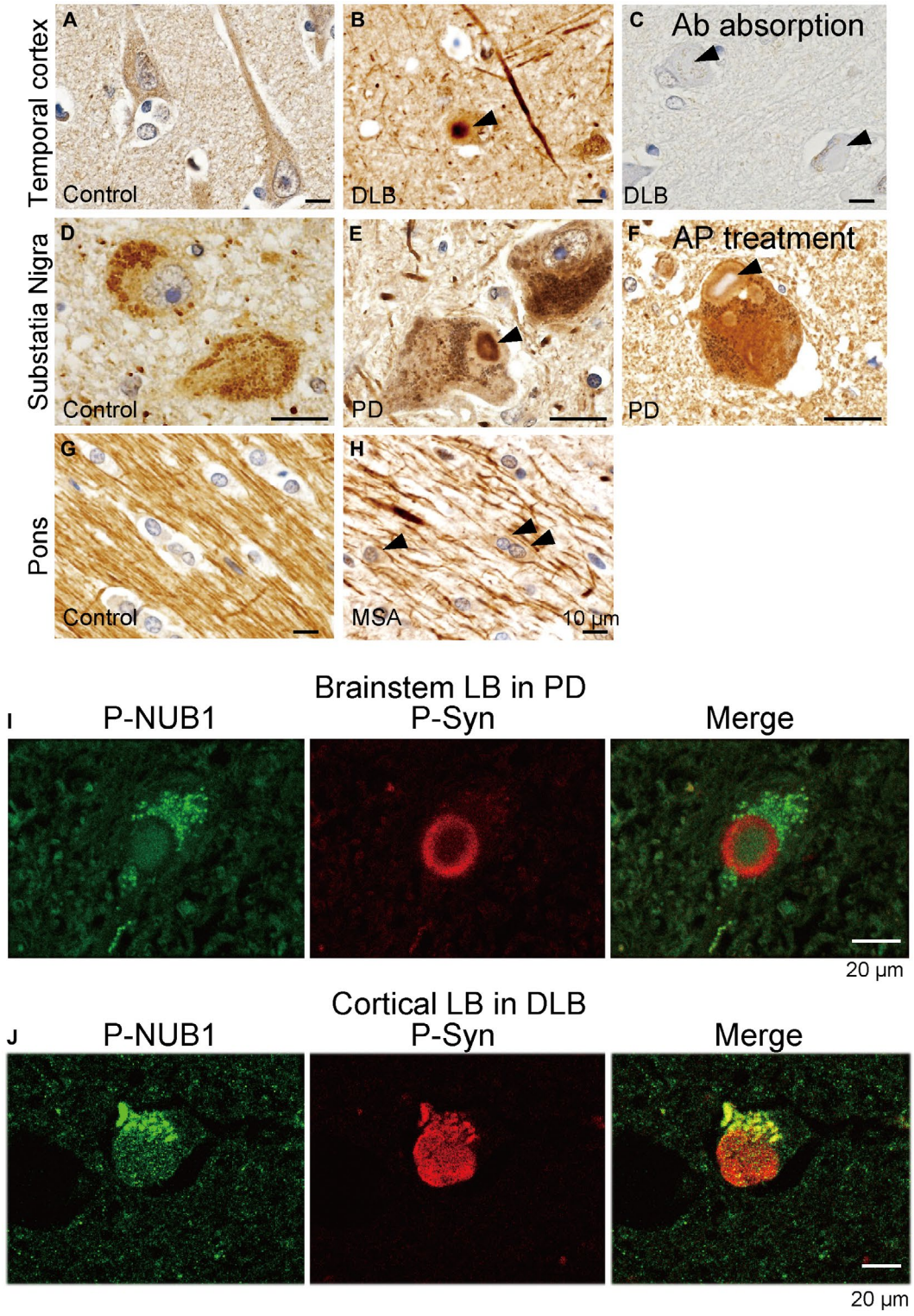

Figure 3. *Immunoreactivity of P-NUB46 in the brain of controls (A, D, G) and patients with PD (E, F), DLB (B, C) and MSA (H).* **A-H.** P-NUB46 immunoreactivity is found in the cytoplasm and dendrites of pyramidal neurons in the temporal cortex (**A**), in the substantia nigra (**D**) and axonal structures in the pons (**G**). P-NUB46 immunoreactivity in cortical Lewy bodies in the temporal lobe (**B**) and brainstem-type Lewy bodies in the substantia nigra (**E**). Anti-P-NUB46 antibody does not react with GCIs (arrowheads in **H**). Antibody (Ab) absorption (**C**) or alkaline phosphatase (AP) pretreatment (**F**) abolishes P-NUB46 immunoreactivity. Bar = 10 µm. **I,J.** Double immunofluorescence demonstrates that anti-P-NUB46 antibody (green) recognizes brainstem-type (**I**) and cortical Lewy bodies (**J**) in PD and DLB, respectively. LBs are positive for phosphorylated α-synuclein (P-Syn) (red). Bar = 20 µm.

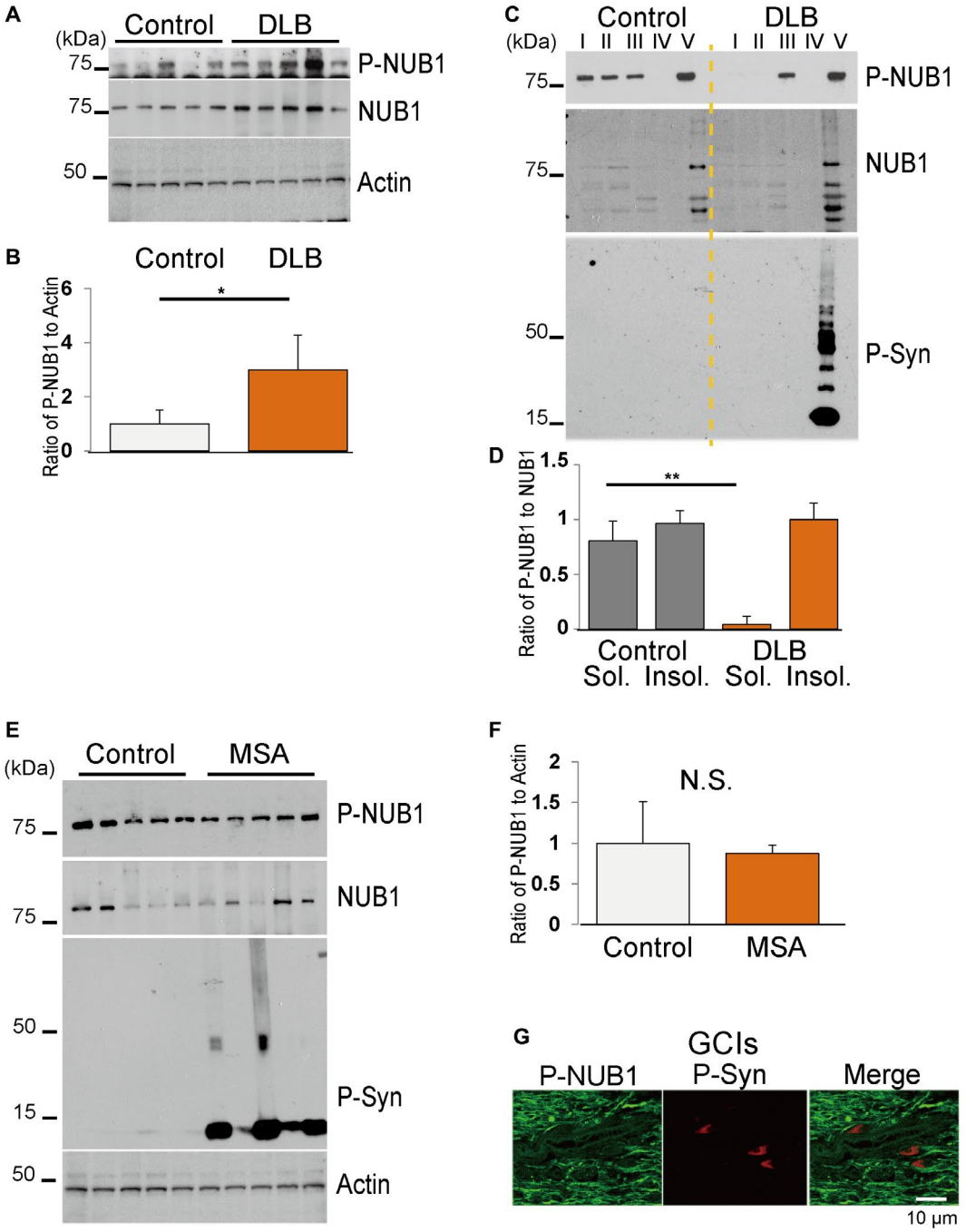

Figure 4. *Increased levels of P-NUB46 in the brains of patients with DLB.* **A.** Frozen tissues were obtained from the temporal cortex of patients with DLB and control subjects (n = 5 in each group) and analyzed by western blot analysis, indicating that P-NUB46 levels are approximately threefold higher in the brains of patients with DLB than those of controls. Data are normalized by actin protein levels in each sample and indicated by mean + SD. The value in controls is defined as 1.0. **B.** Quantitative data of A. $*P < 0.05$, $**P < 0.01$. **C.** Sequential biochemical fractionation shows that P-NUB46 is detected in fractions I, II, III and V in controls, and III and V in DLB. Fractions I and II are Triton X-100 soluble, and III, IV and V are Triton X-100 insoluble. **D.** Quantitative data of C. $*P < 0.05$, $*P < 0.01$. **E.** Equal amounts of lysate from cerebellar white matter of patients with MSA and controls (n = 5 in each group) were analyzed by western blot analysis using antibodies against P-NUB46, pan-NUB1, P-Syn and actin. There are no differences in protein levels of P-NUB46 between MSA and control groups. **F.** Quantification of amounts of E. **G.** Double immunofluorescence demonstrates that anti-P-NUB46 antibody (green) does not recognize GCIs, which are positive for P-Syn (red). Bar = 10 μm.

DISCUSSION

Here, we performed a cell-based assay to screen for the most effective mutant that inhibits aggregation. Among these NUB1 mutants, we found that the NUB S46E mutant exerted the highest inhibitory effect on Htt aggregation. NUB1 possesses a UBL domain at its N-terminus and two or three UBA domains at its C-terminus. We initially predicted that the phosphorylation sites within the UBL or UBA domains play an important role in the degradation of aggregated disease-associated proteins. Because proteins with the UBL/UBA domain share a common property in their ability to interact with 26S proteasomes, they serve as shuttles between ubiquitinated proteins and proteasome (3). Unexpectedly, however, S46 was not localized within the UBL or UBA domain. To investigate the physiological role of P-NUB S46 *in vivo*, we generated phosphorylated specific antibodies against it, and immunohistochemical and biochemical examinations revealed that anti-P-NUB46 antibody reacted with the neuronal cytoplasm, dendrites and axons in the brains of control subjects. Alkaline phosphatase treatment diminished P-NUB46-positive staining, suggesting that NUB1 is physiologically phosphorylated in the brain. Richet *et al* reported that NUB1 interacts with tau protein, which is one of the microtubule-associated proteins (11). Interestingly, the latter authors also demonstrated that NUB1 binds to GSK3β, which is a critical tau kinase, and that NUB1 could modify the ability of tau to bind microtubules through GSK3β activity. Given that the axonal portion is immunostained with anti-P-NUB46 antibody in the white matter in controls and MSA patients, we assume that phosphorylated NUB1 may play an important role in axon structures.

Our previous report demonstrated that NUB1 specifically accumulates in LBs in PD and DLB as well as in GCIs and neuronal cytoplasmic inclusions in MSA (15). To characterize P-NUB46, we pathologically examined the brains of patients with synucleinopathy. Anti-P-NUB46 antibody reacted with LBs in PD and DLB, these results suggest that P-NUB46 plays an important role in aggregate degradation. On the other hands, GCIs in MSA was negative for P-NUB46. Recent studies showed that pathological α-synuclein in LBs and GCIs possesses conformationally and biologically distinct differences. For instance, α-synuclein in GCIs is structurally more compact and is approximately 1000-fold more potent than α-synuclein in LBs during α-synuclein aggregation (9). Regarding transmission efficiency of α-synuclein, α-synuclein in GCIs was more efficiently distributed in the mice brain relative to Syn in LBs (10). Additionally, PK treatment caused different digestive patterns between α-synuclein in LBs and GCIs (9). Considering that pathological α-synuclein in LBs and GCIs is conformationally different, chaperone activity could be involved in the recognition of the tertiary structure of pathological Syn. A NUB1-binding protein, aryl hydrocarbon receptor interacting protein-like 1 (AIPL1), functions as a cochaperone protein in cooperation with a molecular chaperone, Hsp70 (5). In addition, NUB1 also coexists with another molecular chaperone, Hsp90, in fraction with a molecular mass of approximately 443–669 kDa in retinoblastoma cells (5). This raises the possibility that chaperoning machinery containing P-NUB46 recognizes abnormal α-synuclein in LBs through chaperone activity. By contrast, P-NUB46 may fail to react with α-synuclein in GCIs.

P-NUB46 levels were significantly higher in the brains of patients with DLB than in those of controls. Further sequential fractionation revealed that P-NUB46 solubility in DLB was different from that in controls. In fact, Trion X-100-soluble NUB1 completely eliminated in DLB. As shown in Figure 4, pathological α-synuclein is abnormally phosphorylated and becomes insoluble in DLB. Like pathological α-synuclein, we have hypothesized that NUB1 is abnormally phosphorylated and becomes altered in its propensity toward insolubility. Since NUB1 possesses more than 20 potential phosphorylated sites, additional phosphorylation sites should exist in NUB1. In fact, mass spectrometry analysis showed that NUB1 has been identified to be phosphorylated at S485 (21). Further studies will be needed to clarify the mechanism for how kinase/phosphatase is involved in NUB1 and which phosphorylation sites are critical to the pathological status.

In conclusion, we provided evidence that P-NUB46 is highly associated with aggregation, and NUB1 is indeed phosphorylated at S46 in the brain. P-NUB46 levels are significantly higher in DLB patients than in controls. Furthermore, immunostaining showed that LBs are positive for P-NUB S46 whereas GCIs are negative, suggesting that involvement of P-NUB46 seems to be characteristic of LBs, rather than a common phenomenon in α-synuclein-containing inclusions.

ACKNOWLEDGMENTS

This work was supported by JSPS KAKENHI Grant Numbers 17K07089 (to K.T.), 17K07088 (to F.M.) and 18H02533 (to K.W.); the Hirosaki University Institutional Research Grant (to K.W.); The Collaborative Research Project (2018-2810) of Brain Research Institute, Niigata University and Karouji Memorial Fund for Medical Research (to K. T.). The authors wish to express their gratitude to M. Nakata and A. Ono for their technical assistance.

CONFLICT OF INTEREST

The authors have no conflicts of interest to declare.

REFERENCES

1. Fujiwara H, Hasegawa M, Dohmae N, Kawashima A, Masliah E, Goldberg MS *et al* (2002) alpha-Synuclein is phosphorylated in synucleinopathy lesions. *Nat Cell Biol* **4**:160–164.
2. Giasson BI, Duda JE, Murray IV, Chen Q, Souza JM, Hurtig HI *et al* (2000) Oxidative damage linked to

neurodegeneration by selective alpha-synuclein nitration in synucleinopathy lesions. *Science* **290**:985–989.
3. Hartmann-Petersen R, Gordon C (2004) Integral UBL domain proteins: a family of proteasome interacting proteins. *Semin Cell Dev Biol* **15**:247–259.
4. Hasegawa M, Fujiwara H, Nonaka T, Wakabayashi K, Takahashi H, Lee VM *et al* (2002) Phosphorylated alpha-synuclein is ubiquitinated in alpha-synucleinopathy lesions. *J Biol Chem* **277**:49071–49076.
5. Hidalgo-de-Quintana J, Evans RJ, Cheetham ME, van der Spuy J (2008) The Leber congenital amaurosis protein AIPL1 functions as part of a chaperone heterocomplex. *Invest Ophthalmol Vis Sci* **49**:2878–2887.
6. Kito K, Yeh ET, Kamitani T (2001) NUB1, a NEDD8-interacting protein, is induced by interferon and down-regulates the NEDD8 expression. *J Biol Chem* **276**:20603–20609.
7. Lu B, Al-Ramahi I, Valencia A, Wang Q, Berenshteyn F, Yang H *et al* (2013) Identification of NUB1 as a suppressor of mutant Huntington toxicity via enhanced protein clearance. *Nat Neurosci* **16**:562–570.
8. Narain Y, Wyttenbach A, Rankin J, Furlong RA, Rubinsztein DC (1999) A molecular investigation of true dominance in Huntington's disease. *J Med Genet* **36**:739–746.
9. Peng C, Gathagan RJ, Covell DJ, Medellin C, Stieber A, Robinson JL *et al* (2018) Cellular milieu imparts distinct pathological alpha-synuclein strains in alpha-synucleinopathies. *Nature* **557**:558–563.
10. Prusiner SB, Woerman AL, Mordes DA, Watts JC, Rampersaud R, Berry DB *et al* (2015) Evidence for alpha-synuclein prions causing multiple system atrophy in humans with parkinsonism. *Proc Natl Acad Sci U S A* **112**:E5308–E5317.
11. Richet E, Pooler AM, Rodriguez T, Novoselov SS, Schmidtke G, Groettrup M *et al* (2012) NUB1 modulation of GSK3beta reduces tau aggregation. *Hum Mol Genet* **21**:5254–5267.
12. Tanaka T, Kawashima H, Yeh ET, Kamitani T (2003) Regulation of the NEDD8 conjugation system by a splicing variant, NUB1L. *J Biol Chem* **278**:32905–32913.
13. Tanaka T, Yeh ET, Kamitani T (2004) NUB1-mediated targeting of the ubiquitin precursor UbC1 for its C-terminal hydrolysis. *Eur J Biochem* **271**:972–982.
14. Tanji K, Kamitani T, Mori F, Kakita A, Takahashi H, Wakabayashi K (2010) TRIM9, a novel brain-specific E3 ubiquitin ligase, is repressed in the brain of Parkinson's disease and dementia with Lewy bodies. *Neurobiol Dis* **38**:210–218.
15. Tanji K, Mori F, Kakita A, Zhang H, Kito K, Kamitani T *et al* (2007) Immunohistochemical localization of NUB1, a synphilin-1-binding protein, in neurodegenerative disorders. *Acta Neuropathol (Berl)* **114**:365–371.
16. Tanji K, Mori F, Kito K, Kakita A, Mimura J, Itoh K *et al* (2011) Synphilin-1-binding protein NUB1 is colocalized with nonfibrillar, proteinase K-resistant alpha-synuclein in presynapses in Lewy body disease. *J Neuropathol Exp Neurol* **70**:879–889.
17. Tanji K, Mori F, Mimura J, Itoh K, Kakita A, Takahashi H, Wakabayashi K (2010) Proteinase K-resistant alpha-synuclein is deposited in presynapses in human Lewy body disease and A53T alpha-synuclein transgenic mice. *Acta Neuropathol* **120**:145–154.
18. Tanji K, Tanaka T, Mori F, Kito K, Takahashi H, Wakabayashi K, Kamitani T (2006) NUB1 suppresses the formation of Lewy body-like inclusions by proteasomal degradation of synphilin-1. *Am J Pathol* **169**:553–565.
19. Wakabayashi K, Engelender S, Tanaka Y, Yoshimoto M, Mori F, Tsuji S *et al* (2002) Immunocytochemical localization of synphilin-1, an alpha-synuclein-associated protein, in neurodegenerative disorders. *Acta Neuropathol (Berl)* **103**:209–214.
20. Wakabayashi K, Engelender S, Yoshimoto M, Tsuji S, Ross CA, Takahashi H (2000) Synphilin-1 is present in Lewy bodies in Parkinson's disease. *Ann Neurol* **47**:521–523.
21. Williams GR, Bethard JR, Berkaw MN, Nagel AK, Luttrell LM, Ball LE (2015) Exploring G protein-coupled receptor signaling networks using SILAC-based phosphoproteomics. *Methods* **92**:36–50.
22. Zhang HX, Tanji K, Mori F, Wakabayashi K (2008) Epitope mapping of 2E2-D3, a monoclonal antibody directed against human TDP-43. *Neurosci Lett* **434**:170–174.

SUPPORTING INFORMATION

Additional supporting information may be found in the online version of this article at the publisher's web site:

Figure S1. *No difference in age, gender variables and post-mortem interval in hours (PMI) among groups.* **A.** The graph presents age of four groups. **B.** The graph presents gender variable of four groups. **C.** The graph presents PMI of four groups.